Pressure Drop in Gas-Liquid Downflow Through Packed Beds

Pressure-drop in cocurrent gas-liquid downflow through packed beds was experimentally measured for nonfoaming, foaming Newtonian, and non-Newtonian liquids. The variables include the column diameter, packing size and shape, flow rates of the phases, and their physical properties. Unified correlations are presented for the data of the present study as well as data available in literature in terms of Lockhart-Martinelli parameters and flow variables and packing characteristics. The data were modeled using a dynamic interaction model.

P. S. T. Sai, Y. B. G. Varma
Department of Chemical Engineering
Indian Institute of Technology
Madras, 600036, India

Introduction

Gas-liquid contacting is commonly practiced in process equipment to effect the transfer of energy, mass, and/or chemical reaction between the phases. Gas and liquid are often required to flow over a bed of inert or catalytic packing to provide large interfacial area between the phases. When the packing is inert, it serves for intense mixing between the phases, as with absorption followed by homogeneous catalytic reaction in the liquid phase. With solid catalyst for packing, the three-phase system becomes complex with the accompanying additional inter- and intraphysical and chemical transport resistances. The flow of the phases over the packing may be countercurrent or cocurrent, the criterion for the choice of flow often being the throughput and driving force for mass transfer and chemical reaction. Successful modeling of such a system requires a careful study of the hydrodynamics, which includes a knowledge of the flow pattern of the phases and the establishment of correlations for predicting the pressure drop and liquid saturation.

The industrial applications of cocurrent gas-liquid downflow through packed beds include synthesis of butynediol, production of hydrogen peroxide, immobilized enzyme reactions, selective hydrogenation, hydrodesulfurization of petroleum fractions, oxidation of organic compounds in waste water, and treatment of effluent gas.

A rather large number of publications has appeared on the topic covering foaming and especially nonfoaming Newtonian liquids. Excellent reviews are due to Satterfield (1975), Gianetto et al. (1978), Hofmann (1978), Hirose (1978), Shah (1979), Charpentier (1981), Herskowitz and Smith (1983), and Saez and Carbonell (1985). The significant correlations of the earlier investigators are listed in Table 1. While most investigations are limited to the air-water system, the behavior of organic liquids is considered in terms of parameters, λ and ψ accounting for deviations in physical properties from those of the air-water system. Although in actual practice the liquids often exhibit non-Newtonian behavior, there appear to be no data in literature in respect to such liquids.

This paper presents an experimental investigation of the two-phase pressure drop for nonfoaming and foaming Newtonian and non-Newtonian liquids with air in cocurrent downflow through packings differing widely in size, shape, and bed void fraction. The two-phase pressure drop is correlated in terms of flow variables and packing characteristics and Lockhart-Martinelli parameters. The former two require a knowledge of the flow pattern of the phases, while a single correlation in terms of Lockhart-Martinelli parameters is presented for non-foaming Newtonian and non-Newtonian liquids. For foaming liquids, however, the correlation is based on the modified parameter χ'. The dynamic interaction model (Rao et al.., 1983) is simulated and the model parameters are estimated for each of the identified flow regions.

Experimental Method

Experiments were conducted in two different columns covering a wide range in variables as detailed in Table 2. Figure 1 is a schematic diagram of the experimental set-up. Gas and liquid are metered and fed through a distributor at the top of the column to flow cocurrently and to discharge through a separator at the bottom of the column. Pressure taps are provided along the length of the column to measure pressure drop across the chosen length. The two-phase pressure drop per unit length was found

Correspondence concerning this paper should be addressed to Y. B. G. Varma.

Table 1. Earlier Investigations of Two-phase Pressure Drop Correlations

Equation	Reference
Lockhart-Martinelli Parameters	
Nonfoaming system, all hydrodynamic regimes	
(a) $\log\left[\frac{\delta_{lg}}{\delta_l+\delta_g}\right]=\frac{0.416}{(\log\chi)^2+0.666}$	Larkins et al. (1961)
(b1) $\log\left[\frac{\delta_{lg}}{\delta_l+\delta_g}\right]=\frac{0.7}{[\log(\chi/1.2)]^2+1}$	Sato et al. (1975)
(b2) $\phi_l=1.30+1.85\,\chi^{-0.85}$	
(c) $\phi_l=1+\chi^{-1}+1.14\,\chi^{-0.54}$	Midoux et al. (1976)
(d) $\phi_l=1+0.99\,\chi^{-1}+1.14\,\chi^{-0.5}$	Rao et al. (1983)
Foaming system, low interaction regime	
Eq. (c), above	
Foaming System, high interaction regime	
(e) $(\xi_{lg}/\xi_l)^{0.5}=1+(\chi')^{-1}+6.55\,(\chi')^{-0.43}$	Midoux et al. (1976)
Flow Variables and Packing Characteristics	
Nonfoaming system, all hydrodynamic regimes	
(f) $\ln f_{lg}=7.96-1.34\,(\ln z)+0.0021\,(\ln z)^2+0.0078\,(\ln z)^3$	Turpin & Huntington (1967)
(g) $\frac{\Delta P}{h}=4f_t\frac{\rho_l V_l^2}{2gd_p}\left(\frac{1-\epsilon}{\epsilon^3\beta_d^2/\beta_t}\right)$, $f_t=1.2\times10^3\,Re_t^{-1.1}$	Matsuura et al. (1977)
(h) $f_{lg}=A\,(Re_l^b/Re_g^c)\,\eta^{0.75}$	Rao et al. (1983)

Flow Regime*	A	b	c
GCF	4.6×10^3	0.4	1.05
PF	5.4×10^3	0.7	1.30
DBF	4.6×10^3	1.05	1.60

Equation	Reference
Nonfoaming and foaming systems, low interaction regime	
(--) $\delta_{lg}=K_l\frac{[1-\epsilon(1-\beta_s-\beta_d)]^2}{\epsilon^3(1-\beta_s-\beta_d)^3}\cdot\mu_g V_g+k_2\frac{[1-\epsilon(1-\beta_s-\beta_d)]}{\epsilon^3(1-\beta_s-\beta_d)^3}\cdot\rho_g V_g^2$	Specchia & Baldi (1977)
Nonfoaming and foaming systems, high interaction regime	
(--) $\ln f_{lg}=7.82-1.3\ln(Z/\psi^{1.1})-0.0573\ln[(Z/\psi^{1.1})]^2$	Specchia & Baldi (1977)

*GCF, gas-continuous flow; PF, pulse flow; DBF, dispersed bubble flow

to vary, decreasing from the top to the bottom of the column. The pressure drop across section II for column I and over the entire length for column II were chosen for purposes of data analysis.

The effective particle diameter, defined as $d_p = 6V_p/S_p$, is the diameter of a sphere having the same volume-to-surface area as the particle (Foust et al., 1960). The column-to-particle diameter varies in the present study from 4.7 to 29, Table 2; due care is taken, however, in the design of the gas and liquid distributor to avoid any uneven distribution of fluids in the bed.

Table 3 lists the physical properties of the liquids used in the present study. Since the liquids are prepared at different times for each experimental scheme, as for example for a change in packing type, a variation in their physical properties is sometimes noted, as reported in Table 3.

Results and Discussion

Figures 2 to 6 present typical variations in pressure drop measured under different experimental conditions. The two-phase pressure drop increases with increase in the flow rate of either of the phases, Figures 2 and 3. It is independent of column diameter but decreases with increase in either effective particle diameter or bed void fraction, Figures 2 and 4.

The two-phase pressure drop shows a maximum of three distinct types of functional dependency, corresponding to gas-continuous flow (trickle flow and spray flow), pulse flow, and dispersed bubble flow for nonfoaming Newtonian and non-Newtonian liquids, Figures 2 and 3. Foaming liquids exhibit foaming pulse flow and foaming flow instead of dispersed bubble flow, Figure 5. The transition from gas-continuous to pulse flow occurs at a high liquid rate as the gas rate is increased, Figures 2 and 3, which is also true of the transition from pulse flow to dispersed bubble flow or to foaming pulse flow. The two-phase pressure drop increases with increase in liquid viscosity for Newtonian liquids or in the flow consistency index for non-Newtonian liquids, Figure 6.

Two principal types of correlations are given in the literature to correlate the two-phase pressure drop. The first of these uses the dimensionless parameters ϕ_l and χ originally used by Lockhart and Martinelli (1949) for two-phase flow in horizontal pipes. The second relates the pressure loss to the flow rate of the

Table 2. Range of Variables Investigated in Present Study

	Column I			Column II		
Diameter, m	92.4×10^{-3}			25.0×10^{-3}		
Packing height, m	1.835			0.508		
Test section, m	0.4, 0.5, 0.6			0.45		
Flow rates, kg · m^{-2} · s^{-1}						
Liquid	4.3–50.0			3.0–58.8		
Air	0.18–1.54			0.17–2.32		
Packings, linear dimension, m*	Size $\times10^{-3}$	$d_p\times10^{-3}$	ϵ	Size $\times10^{-3}$	$d_p\times10^{-3}$	ϵ
Spheres	11.72	11.72	0.392	4.32	4.32	0.409
Spheres	6.72	6.72	0.351	2.39	2.39	0.389
Cylinders, $d\times h_p$	8.18×7.91	8.09	0.345	5.08×5.71	5.27	0.385
Raschig rings, $d_i\times d_o\times h_p$	$7.46\times9.62\times10.32$	3.14	0.720	$4.36\times5.53\times6.1$	1.59	0.720

*d, particle diameter; h_p, particle height; i, o, inside, outside dimensions

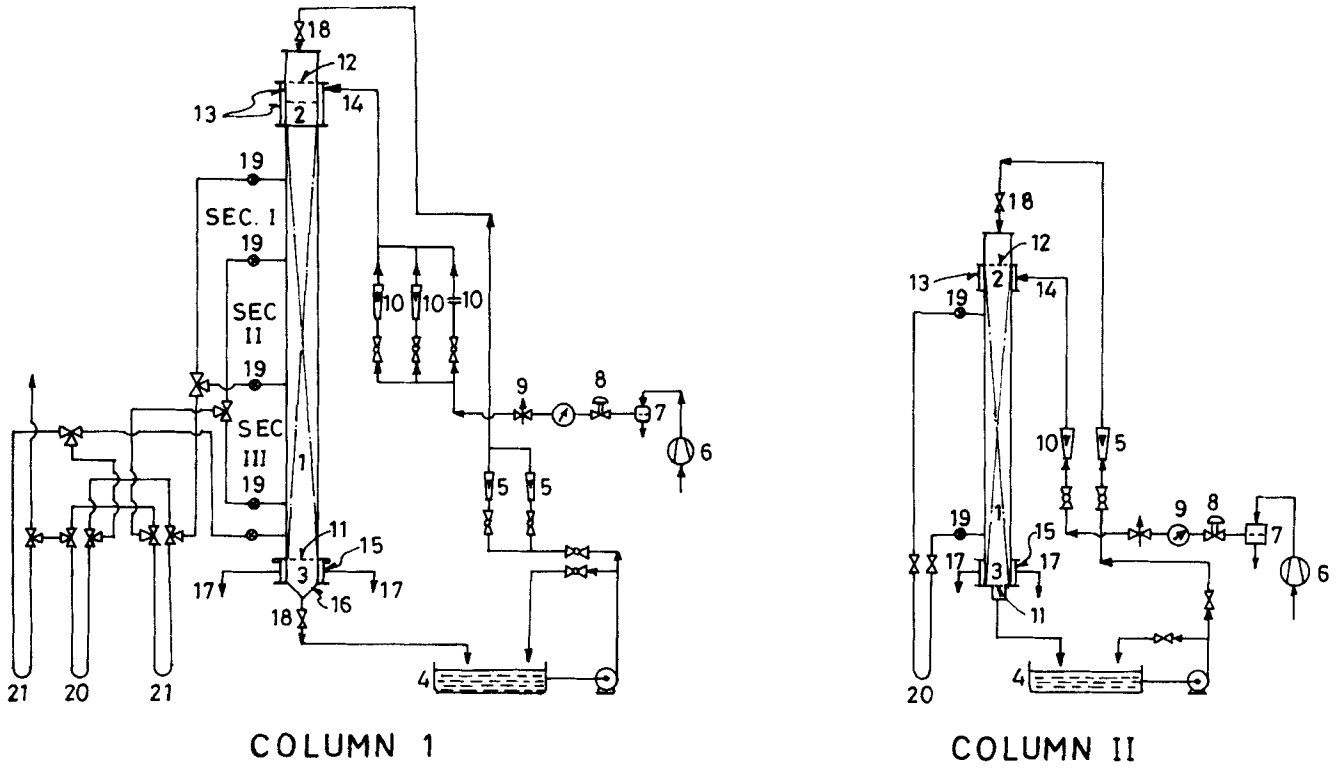

Figure 1. Diagram of experimental set-up.

1. Packed section
2. Distributor
3. Discharger
4. Liquid tank
5. Low/high range flow meters for liquid
6. Compressor
7. Air filter
8. Pressure regulator
9. Control valve
10. Low/high range flow meters for air
11. Grid plate
12. Brass plate
13. Concentric cylinders
14. Radial feed inlets for air
15. Concentric perspex tubes
16. Brass conical section
17. Outlet tubes for air
18. Quick-closing valves
19. Gas-liquid separators
20. Mercury manometers
21. Carbon tetrachloride manometers

Table 3. Physical Properties of Liquids Used in Present Study

Liquid	ρ kg/m^3	$\mu \times 10^3$ N · s/m^2	$\sigma \times 10^3$ N/m
Newtonian Liquids			
Water	996	0.850	72
10% glycerine	1,026	1.145	68
20% glycerine			
4.32 mm spheres	1,048	1.523	62
2.39 mm spheres	1,048	1.146	62
5.27 mm cylinders	1,048	1.607	62
1.59 mm Raschig rings	1,048	1.399	62
40% glycerine			
4.32 mm spheres	1,107	3.310	55
5.27 mm cylinders	1,107	3.582	55
1.59 mm Raschig rings	1,107	3.416	55
Kerosene	787	1.322	33
n-Hexane	663	0.344	22

Liquid*	n	$K \times 10^3$ kg/m · s^{2-n}	ρ kg/m^3	$\sigma \times 10^3$ N/m
Non-Newtonian Liquids				
0.1% CMC	0.967	1.61	996	72
0.2% CMC	0.856	3.97	1,000	72
0.5% CMC	0.789	10.27	1,001	70
1.0% CMC	0.735	18.34	1,004	66
2.0% CMC	0.785	62.43	1,010	55

*CMC, carboxymethyl cellulose

phases or their respective Reynolds numbers and bed void fraction either for the entire region of operation or separately for each identified flow region. The correlations relating ϕ_l and χ were successfully adopted by Larkins et al. (1961), Weekman and Myers (1964), Sato et al. (1973), Midoux et al. (1976), and Rao et al. (1983), and in a modified form by Charpentier and coworkers (1969, 1971, 1976). The correlations relating the friction factor directly in terms of flow variables for the entire range of operation was attempted by Turpin and Huntington (1967). Specchia and Baldi (1977) differentiated the low interaction regime from the high interaction regime and related the pressure loss in the former regime in terms of liquid saturation and in the high interaction regime in terms of two dimensionless parameters, Z and ψ, the former being the ratio of gas and liquid Reynolds numbers and the latter accounting for the deviation in the physical properties of the liquid from that of water. Subsequently Rao et al. (1983) related the friction factor in terms of gas and liquid Reynolds numbers and the bed void fraction for each of the three identified flow regions for the air-water system.

Correlations in terms of flow variables and packing characteristics

The two-phase pressure drop measured in the present study using Newtonian liquids is correlated in terms of the flow vari-

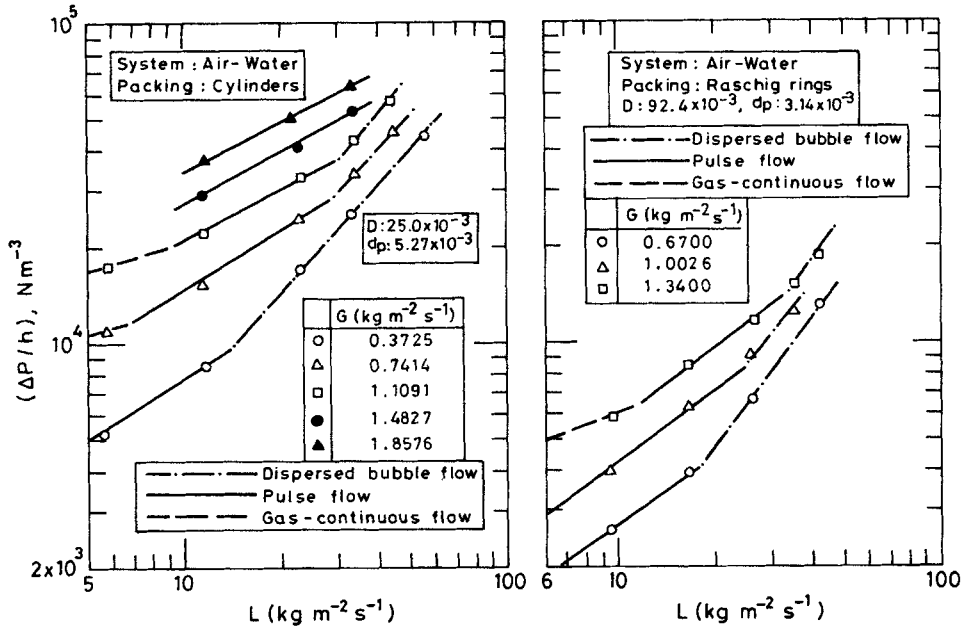

Figure 2. Typical variation in pressure drop with system variables.

ables and packing characteristics as below:

Gas-continuous flow (nonfoaming and foaming systems)

$$F = 1{,}320\left(\frac{Re_g}{Re_l}\right)^{1.0}\left(\frac{\sigma_w}{\sigma_l}\right)^{0.05}\left(\frac{\mu_w}{\mu_l}\right)^{1.4}\left(\frac{\rho_l}{\rho_w}\right)^{1.3} \quad (1)$$

Pulse flow (nonfoaming and foaming systems)

$$F = 1{,}950\left(\frac{Re_g}{Re_l}\right)^{0.7}\left(\frac{\sigma_w}{\sigma_l}\right)^{0.05}\left(\frac{\mu_w}{\mu_l}\right)^{1.1}\left(\frac{\rho_l}{\rho_w}\right)^{1.3} \quad (2)$$

Dispersed bubble flow (nonfoaming systems)

$$F = 2{,}035\left(\frac{Re_g}{Re_l}\right)^{0.4}\left(\frac{\sigma_w}{\sigma_l}\right)^{0.05}\left(\frac{\mu_w}{\mu_l}\right)^{0.8}\left(\frac{\rho_l}{\rho_w}\right)^{1.3} \quad (3)$$

Foaming pulse flow (foaming systems)

$$F = 3{,}100\left(\frac{Re_g}{Re_l}\right)^{0.35}\left(\frac{\sigma_l}{\sigma_w - \sigma_l}\right)^{0.1}\left(\frac{\mu_w}{\mu_l}\right)^{0.9}\left(\frac{\rho_l}{\rho_w}\right)^{1.3} \quad (4)$$

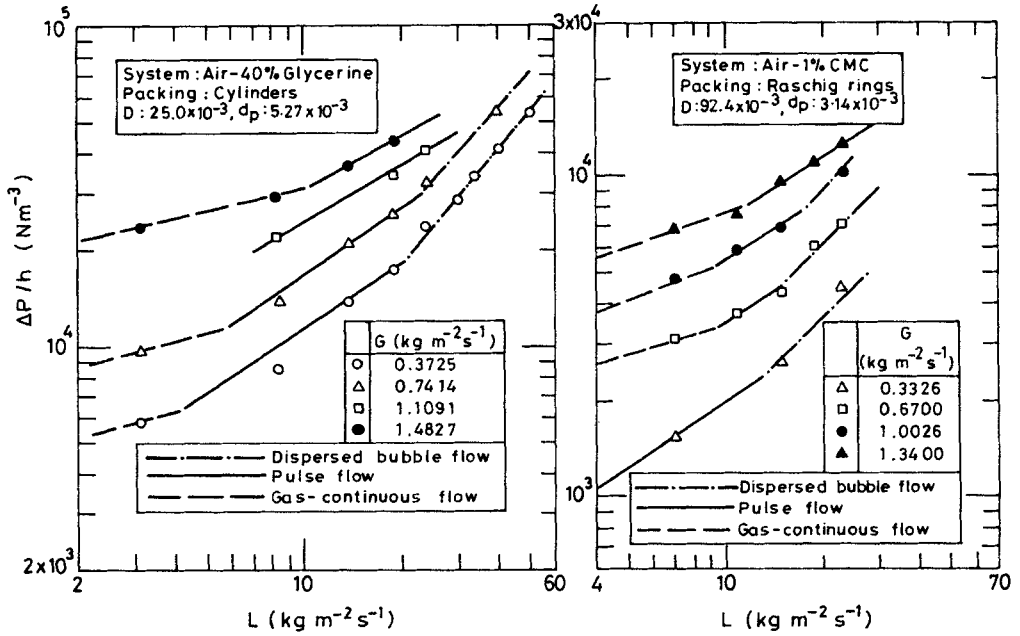

Figure 3. Typical variation in pressure drop with system variables.

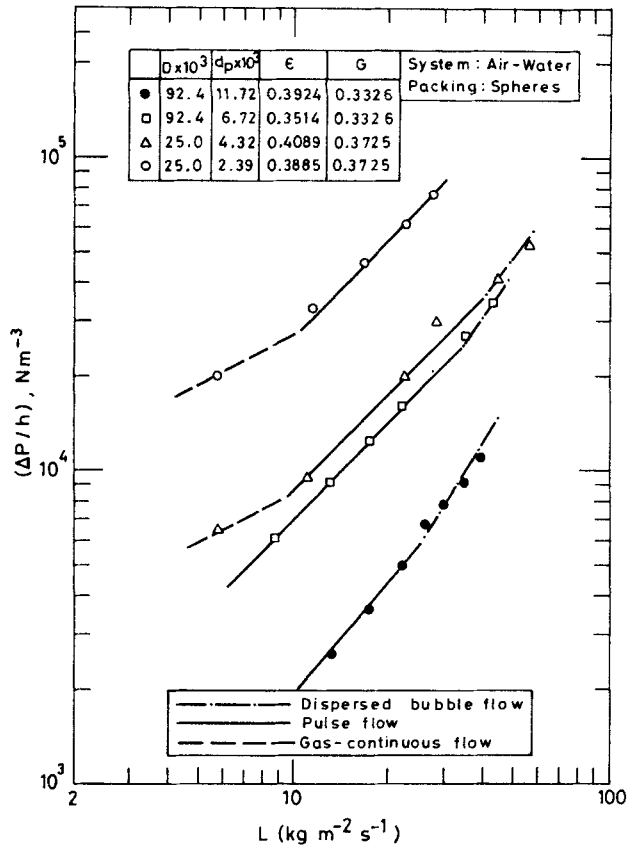

Figure 4. Typical variation in pressure drop with system variables: effect of packing size.

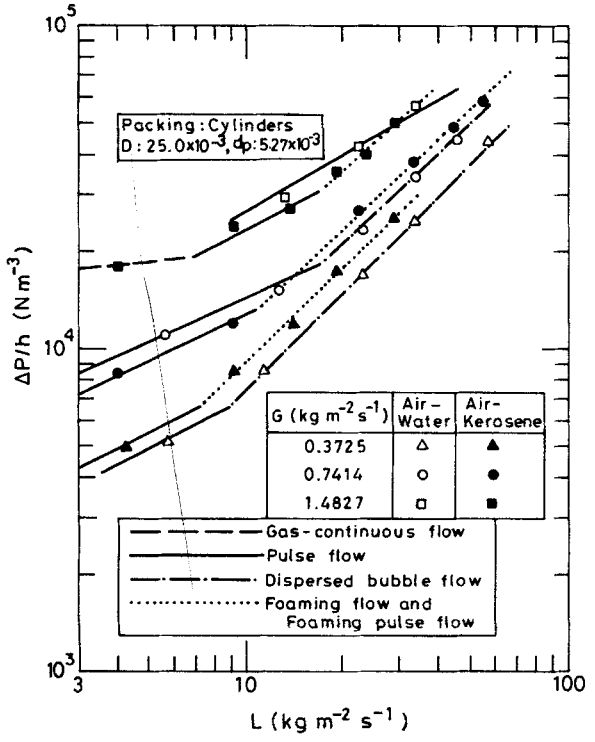

Figure 5. Typical variation in pressure drop with system variables, foaming and nonfoaming liquids.

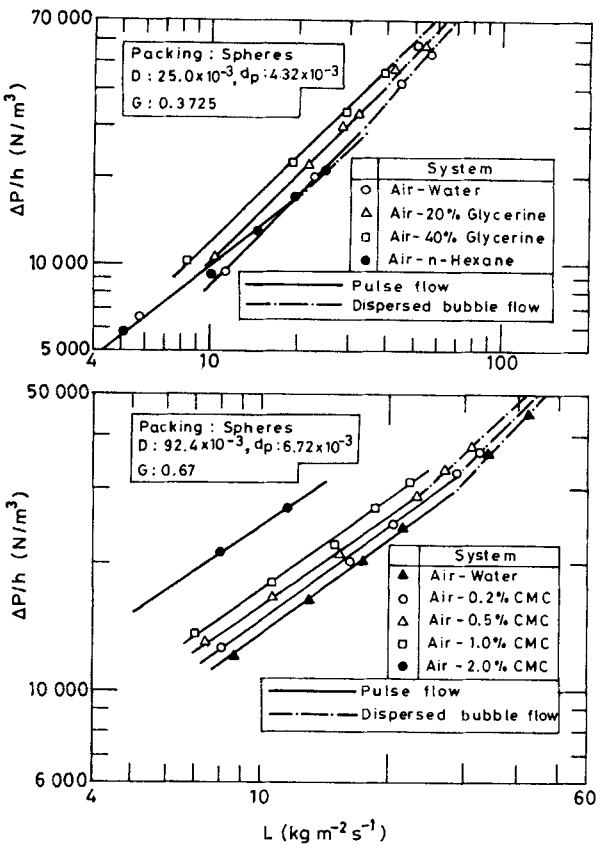

Figure 6. Typical variation in pressure drop with system variables: effect of physical properties of liquids.

Foaming flow (foaming systems)

$$F = 3{,}670\left(\frac{Re_g}{Re_l}\right)^{0.35}\left(\frac{\sigma_l}{\sigma_w - \sigma_l}\right)^{0.1}\left(\frac{\mu_w}{\mu_l}\right)^{1.0}\left(\frac{\rho_l}{\rho_w}\right)^{2.0} \tag{5}$$

where $F = f_c Re_1^{0.6}/\eta^{0.75}$.

The ratio of the physical properties of the fluids to those of water, as represented in the above equations, is consistent with the representations of the earlier investigators (Charpentier and Favier, 1975; Specchia and Baldi, 1977). The friction factor f_c predicted using Eqs. 1–5 is satisfactorily compared with the experimental value f_e, defined as

$$f_e = 2\Delta P_{lg} d_p/\rho_l V_l^2 h$$

The mean relative quadratic error, σ, between the predicted (X_c) and the experimental (X_e) parameter values, defined as

$$\sigma = \sqrt{\sum_i^N [(X_{c,i} - X_{e,i})/X_{e,i}]^2/(N-1)}$$

is listed in Table 4 for the experimental data obtained in the present study. A typical comparison of f_c and f_e for a nonfoaming system is illustrated in Figure 7.

The correlations for the pressure drop using nonNewtonian

Table 4. Comparison of Experimental and Predicted Parameters

Eq. No.	Flow Regime*	Parameter	No. of Data	Mean Rel. Quad. Error σ
Newtonian nonfoaming system				
1	GCF	f	48	0.12
2	PF	f	257	0.15
3	DBF	f	96	0.15
Newtonian foaming system				
1	GCF	f	14	0.12
2	PF	f	65	0.12
4	FPF	f	58	0.15
5	FF	f	50	0.11
Non-Newtonian nonfoaming system				
6	GCF	f_M	44	0.13
7	PF	f_M	377	0.19
8	DBF	f_M	196	0.14
Newtonian nonfoaming system, Lockhart-Martinelli correlation				
9	—	ϕ_l	401	0.13
Newtonian foaming system, Lockhart-Martinelli correlation				
10	—	ϕ_l	173	0.15
Non-Newtonian nonfoaming system, Lockhart-Martinelli correlation				
11	—	ϕ_l	617	0.15
Newtonian nonfoaming system, Eqs. A, B, text				
—	GCF	$\Delta P/h$	25	0.12
—	PF	$\Delta P/h$	57	0.12
—	DBF	$\Delta P/h$	55	0.12
Newtonian foaming system, Eqs. A, B, text				
—	GCF	$\Delta P/h$	9	0.07
—	PF	$\Delta P/h$	39	0.13
—	FPF/FF	$\Delta P/h$	35	0.11
Non-Newtonian nonfoaming system				
—	GCF	$\Delta P/h$	21	0.12
—	PF	$\Delta P/h$	43	0.13
—	DBF	$\Delta P/h$	41	0.12

*GCF, gas-continuous flow; PF, pulse flow; DBF, dispersed bubble flow; FPF, foaming pulse flow; FF, foaming flow

liquids are as below:

Gas-continuous flow

$$F_M = 0.05\left(\frac{Re_g}{Re_M}\right)^{1.0}\left(\frac{1}{K^{1.4}}\right) \tag{6}$$

Pulse flow

$$F_M = 0.073\left(\frac{Re_g}{Re_M}\right)^{0.7}\left(\frac{1}{K^{1.1}}\right) \tag{7}$$

Dispersed bubble flow

$$F_M = 7.5\left(\frac{Re_g}{Re_M}\right)^{0.4}\left(\frac{1}{K^{0.8}}\right) \tag{8}$$

where $F_M = f_{Mc}Re_M^{0.6}/\eta_M^{0.75}$.

The constants in Eqs. 6–8 have units consistent with the flow behavior index raised to the appropriate power. Figure 8 compares the friction factor f_{Mc} with the experimental friction factor defined as

$$f_{Me} = (2\Delta P_{lg}d_p/\rho_l V_l^2 h)[(2n+1)/(3n+1)]$$

Equations 6–8 reduce to Eqs. 1–3 for the air-water system provided $n = 1$ and viscosity is substituted for flow consistency index. Equations 1–8 require *a priori* knowledge of the flow pattern of the phases, to predict the two-phase pressure drop. The flow region may be discriminated approximately from the ratio of the liquid to the gas flow rate as below:

	L/G Ratio for Flow Region Discrimination			
	Gas-Continuous Flow	Pulse Flow	Dispersed Bubble/ Foaming Pulse Flow	Foaming Flow
Newtonian nonfoaming	<4	10–40	>80	—
Newtonian foaming	<4	5–25	25–50	>150
Non-Newtonian	<4	10–25	>40	—

Correlations in terms of Lockhart-Martinelli parameters

Defining ϕ_{le} and χ as

$$\phi_{le} = (\Delta P_{lg}/\Delta P_l)^{1/2}; \quad \chi = (\Delta P_l/\Delta P_g)^{1/2}$$

the experimental data of the present study are correlated thus:

All regions of flow (Newtonian nonfoaming system)

$$\phi_l = 1.25\left(\frac{\epsilon}{1-\epsilon}\right)^{1/2} + \frac{1}{\chi} + \frac{1.15}{\sqrt{\chi}} \tag{9}$$

Equation 9 is also valid for trickle flow in foaming fluids.

Pulse flow, foaming pulse flow, and foaming flow (Newtonian foaming systems)

$$\phi_l' = 1 + \frac{1}{\chi'} + \frac{6.55}{(\chi')^{0.43}}\left(\frac{\epsilon}{1-\epsilon}\right)^{1/2} \tag{10}$$

All regions of flow (non-Newtonian systems)

$$\phi_l = 1.25\,n\left(\frac{\epsilon}{1-\epsilon}\right)^{1/2} + \frac{1}{\chi} + \frac{1.15}{\sqrt{\chi}} \tag{11}$$

Figure 9 compares ϕ_l, predicted as above using Eq. 11 with ϕ_{le} obtained using the experimental ΔP_{lg}. ΔP_l is calculated using the equation due to Kemblowski and Mertl (1974) suggested for Stokesian fluids flowing through packed beds, while ΔP_g is calculated using the Ergun (1952) equation. The mean relative quadratic error, σ, is listed in Table 4 for the correlations based on Lockhart-Martinelli parameters, Eqs. 9–11.

The correlation due to Rao et al. (1983) (Eq. d, present Table 1) predicts low pressure drop across the bed for packings of high bed void fraction (Raschig rings, Figure 10), necessitating the incorporation of ϵ as an additional term in Eq. d to give Eq. 9.

The study of the pressure drop for a foaming system is principally due to Midoux et al. (1976), who represented their data in

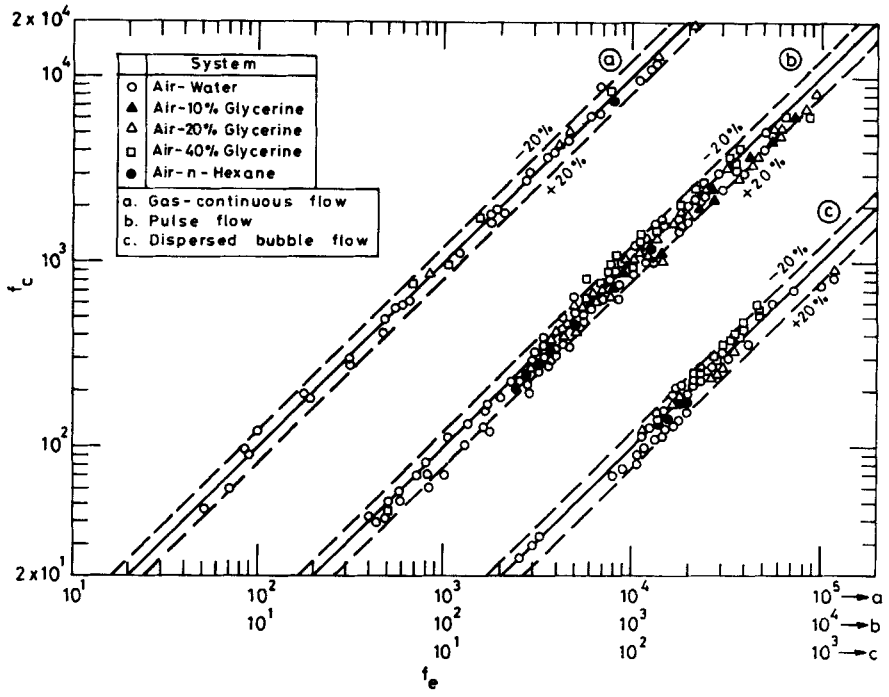

Figure 7. Experimental and predicted friction factor, nonfoaming system.

terms of modified Lockhart-Martinelli parameters in the high interaction regime. However, as with a nonfoaming system, the correlation (Eq. e, Table 1)—predicts less pressure drop compared to the measured value for Raschig rings, necessitating once again the use of ϵ in correlating the experimental data using Eq. 10. It may be noted that these packings (Raschig rings) give rise to high interfacial area per unit volume as compared to packings of spheres or cylinders. Further, Rao et al. (1981) noted that the transitional liquid and gas flow rates from one region to another, as well as the extent of the pulse flow region, are different for Raschig rings compared to spheres or cylinders. A kerosene-air system gave rise to foaming with all packings, whereas 20 and 40% glycerine solutions gave foaming with Raschig rings only. Specchia and Baldi (1977) listed 9 and 29% glycerine solutions as foaming liquids while Talmor (1977) listed glycerine solutions as nonfoaming liquids.

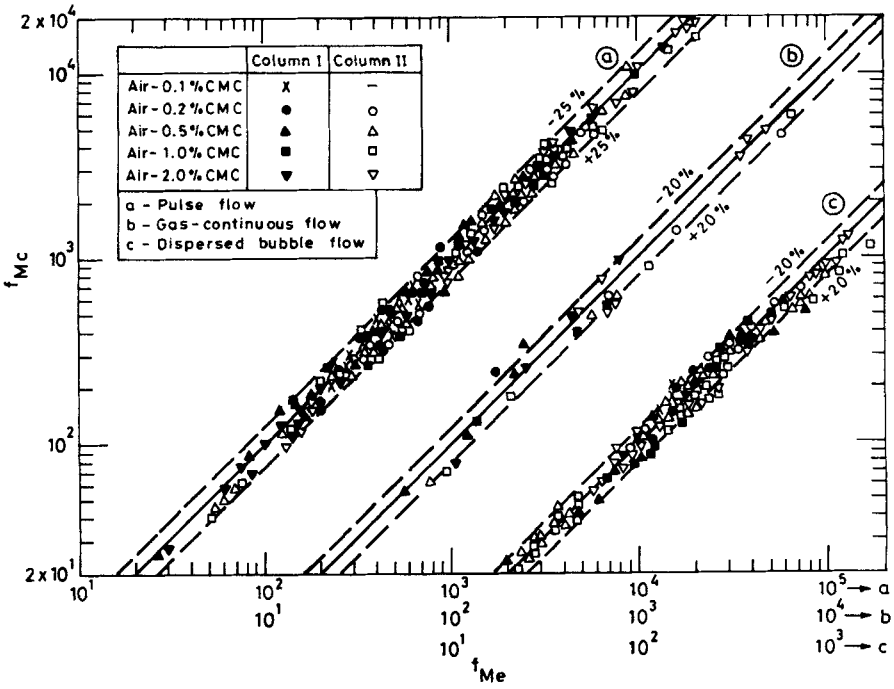

Figure 8. Experimental and predicted friction factor, non-Newtonian system.

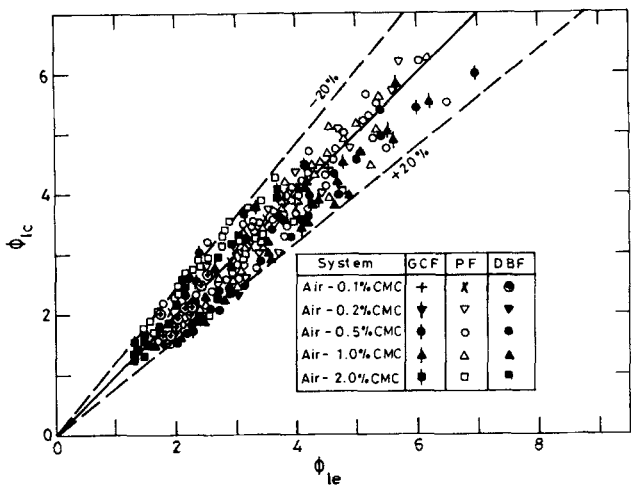

Figure 9. Experimental and predicted two-phase pressure drop, non-Newtonian system.

It is significant to note that the pressure drop for Newtonian nonfoaming and non-Newtonian liquids obeying the power law is characterized through the same functional relationship bearing Lockhart-Martinelli parameters.

The Model

The experimental two-phase pressure drop of the present study is matched with the dynamic interaction model of Rao et al. (1983). The dynamic interaction model is a modification of the geometric interaction model originally proposed by Sweeney (1967), and includes additional pressure drop due to formation, breakage, and reformation of bubbles. The model has nine parameters α_l, α_g, and α_b for each of the three identified flow regions: gas-continuous flow, pulse flow, and dispersed bubble flow. The factors α_l and α_g are the ratios of the equivalent area of contact between the phases (liquid and gas, respectively) and packing in two-phase flow to that in single-phase flow. α_b is a nonideality factor accounting for the fact that in practice bubbles may not break or reform quite so often, and is expected to assume values between 0 and 1. At low liquid flow rates corresponding to gas-continuous flow, the liquid saturation is unaffected by the gas flow rate and thus $\alpha_l = 1$, provided the gas flow rate is not too high to cause significant entrainment. It can likewise be further assumed that $\alpha_g = 1$ and $\alpha_b = 0$, since there is no bubble formation in this region.

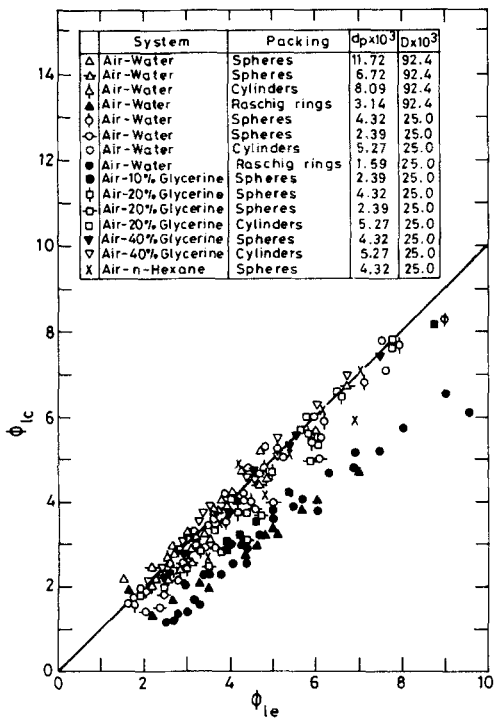

Figure 10. Experimental two-phase pressure drop data compared with correlation of Rao et al. (1983).

At intermediate and high liquid flow rates the gas flow reduces liquid saturation. At low gas flow rates corresponding to dispersed bubble flow, the formation and coalescence of bubbles lead to filling up of many of the voids and thus reduce the contact area between the packing and the liquid when compared with single-phase flow. It is assumed in this region that this reduction is equal to the liquid saturation itself, that is, $\alpha_l = \beta_t$. α_g should be large in this region, as bubbles increase the interfacial area for frictional losses. α_b should be maximum and lies between 0 and 1. α_g and α_b are obtained by fitting the experimental data with the model equations.

The pulse flow is characterized by alternate pulses of low and high density. The bubble formation in the high density pulse reduces α_l, although this reduction is less than in dispersed bubble flow. The increased gas flow rate, however, causes spreading of the liquid film over a large area of packing. The effect of bubbles will be more significant in reducing α_l. By trial and error, a value of 0.75 for α_l was assigned to give predictions in agreement with experiment (Rao et al., 1983). The values of α_g and α_b should be less than those for dispersed bubble flow. Thus, of the nine parameters in the model, values are assigned *a priori* to five parameters as follows:

$\alpha_l = 1.0; \quad \alpha_g = 1.0; \quad \alpha_b = 0$	Gas-continuous flow
$\alpha_l = 0.75$	Pulse flow
$\alpha_l = \beta_t$	Dispersed bubble flow

Rao et al. (1983) dealt in detail with the model for the air-water system. The model equations are:

$$\delta_{lg} - \beta_t - \alpha_l \frac{\delta_l}{\beta_t^3} + 1 = 0 \tag{A}$$

$$\delta_{lg} - \beta_t + \gamma_l + \gamma_g \frac{\rho_g}{\rho_l} - \left[\alpha_g \frac{\delta_g}{(1-\beta_t)^3} + \alpha_b (6S)^{2/3} \cdot (1.5\delta_{lg}^{-1})^{1/3}(d_0/d_p)\right]\gamma_g - \alpha_l \frac{\delta_l}{\beta_t^3}\gamma_l = 0 \tag{B}$$

The liquid saturation, β, is calculated from Eq. A using the experimental pressure drop. Then a linear least-squares analysis of Eq. B using experimental δ_{lg} and the calculated β gives the

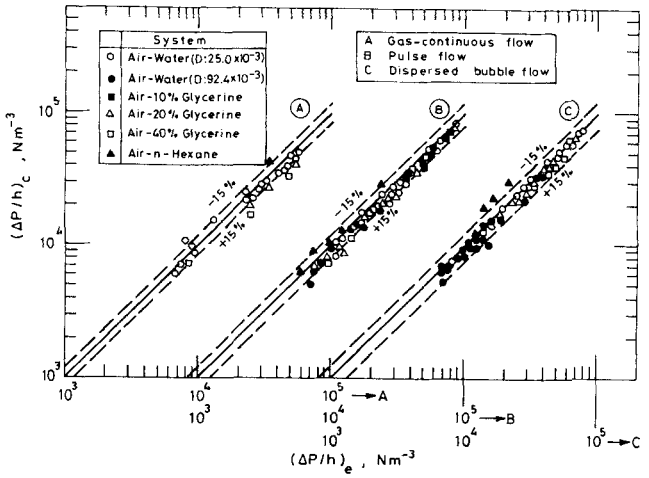

Figure 11. Experimental two-phase pressure drop compared with model prediction, nonfoaming system.

following values for the parameters:

	Pulse Flow		Dispersed Bubble Flow	
	$\alpha_g \times 10^3$	α_b	$\alpha_g \times 10^3$	α_b
Newtonian nonfoaming system	1.55	0.117	3.25	0.140
Newtonian foaming system	1.59	0.046	2.80	0.122
Non-Newtonian system	0.91	0.088	2.00	0.108

α_g, listed above, is about 1,000 times smaller than that reported earlier by Rao et al. (1983) for the air-water system. This is due to a variation in the definition of $\delta_g (=\Delta P_g/\rho_g g)$ effected in the present study, while Rao et al. defined $\delta_g = \Delta P_g/\rho_l g$.

Figure 11 compares the experimental two-phase pressure drop for a Newtonian nonfoaming system with the pressure drop predicted using the model for each of the identified flow regions and for the systems covered in the present study. The mean relative quadratic error, σ, is listed in Table 4 for comparison of the model with the experimental data of the present study.

Notation

d_o = characteristic length = $(D - Nd_p)/N$, m
d_p = effective particle diameter, m
D = column diameter, m
g = acceleration due to gravity, m · s^{-2}
G = gas superficial mass velocity, kg · m^{-2} · s^{-1}
h = height of test section, m
K = flow consistency index, kg · m^{-1} · s^{n-2}
L = liquid superficial mass velocity, kg · m^{-2} · s^{-1}
n = flow behavior index
N = integer = $(D/d_p) - 1$
ΔP = pressure drop, $N \cdot m^{-2}$
V = superficial velocity of the phase, m · s^{-1}
V_p = particle volume, m^3
S = free cross-sectional area
S_p = particle surface area, m^2

Greek letters

α = model parameter used by Rao et al. (1983)
β = liquid saturation
ϵ = bed void fraction
μ = viscosity, N · s · m^{-2}
ρ = density, kg · m^{-3}
σ = surface tension, N · m^{-1}

Dimensionless parameters/groups

$f = 2\Delta P_{lg} d_p/\rho_l V_l^2 h$
$f_M = [2\Delta P_{lg} d_p/\rho_l V_l^2 h][(2n + 1)/(3n + 1)]$
$Re = d_p \rho V/\mu$
$Re_M = d_p^n V_l^{2-n} \rho_l / K$
$Re_t = d_p V \rho_l/\mu_l (1 - \epsilon)(\beta_d/\beta_t)$
$Z = Re_g^{1.167}/Re_l^{0.767}$
$\xi_g = \{(G/\epsilon)[(1/\rho_g)(\Delta H/h)_g + (1/\rho_e)]\}$
$\xi_l = \{(L/\epsilon)[(1/\rho_l)(\Delta H/h)_l + (1/\rho_e)]\}$
$\xi_{lg} = ((1/\epsilon)\{[(L/\rho_l) + (G/\rho_g)](\Delta H/h)_{lg}\} + [(L + G)/\epsilon\rho_e])$
$\gamma_l = (L/\rho_l)/[(L/\rho_l + (G/\rho_g)]$
$\gamma_g = 1 - \gamma_l$
$\delta = \Delta P/\rho_{gh}$
$\phi_l = (\delta_{lg}/\delta_l)^{1/2}$
$\phi_l' = (\xi_{lg}/\xi_l)$
$\chi = (\delta_l/\delta_g)^{1/2}$
$\chi' = (\xi_l/\xi_g)^{1/2}$
$\psi = (\sigma_w/\sigma_l)[(\mu_l/\mu_w)(\rho_w/\rho_l)^2]^{1/3}$
$\psi_M = (\sigma_w/\sigma_l)[(K/\mu_w)(\rho_w/\rho_l)^2]^{1/3}$
$\eta = (1 - \epsilon)^2/\epsilon^3$
$\eta_M = (1 - \epsilon)^{n+1}/\epsilon^{2n+1}$
$\lambda = [(\rho_g/\rho_{air})(\rho_l/\rho_w)]^{1/2}$

Subscripts

c = predicted
d = dynamic
e = experimental
g = gas-phase
l = liquid-phase
lg = two-phase
s = static
t = total
w = water

Abbreviations

CMC = carboxymethyl celluose
DBF = dispersed bubble flow
F = foaming
FF = foaming flow
FPF = foaming pulse flow
GCF = gas continuous flow
NF = nonfoaming
PF = pulse flow
TF = trickle flow
SF = spray flow

Literature Cited

Charpentier, J. C., in *Advances in Chemical Engineering*, T. B. Drew et al., eds., Academic Press (1981).

———, "Recent Progress in the Phase Gas-Liquid Mass Transfer in Packed Bed," *Chem. Eng. J.*, **11**, 161 (1976).

Charpentier, J. C., and M. Favier, "Some Liquid Holdup Experimental Data in Trickle-Bed Reactors for Foaming and Nonfoaming Hydrocarbons," *AIChE J.*, **21**, 1213 (1975).

Charpentier, J. C., M. Bakos, and P. LeGoff, "Hydrodynamics of Two-Phase Concurrent Downflow in Packed-Bed Reactors," 2nd Cong. Quelques Applications de la Chimie Physique, Veszprem, Hungary (1971).

Charpentier, J. C., C. Prost, and P. LeGoff, "Chute de Pression pour des Ecoulements a Cocurrent et a Contrecourant dans les Collonnes a Garnissage Arrose: Comparaison avec le Garnissage Noye," *Chem. Eng. Sci.*, **24**, 1777 (1969).

Ergun, S., "Fluid Flow Through Packed Columns," *Chem. Eng. Prog.*, **2**, 89 (1952).

Foust, A. S., L. A. Wenzel, C. W. Clump, L. Maus, and L. B. Andersen, *Principles of Unit Operations*, Wiley, New York (1960).

Gianetto, A., G. Baldi, V. Specchia, and S. Sicardi, "Hydrodynamics and Solid-Liquid Contacting Effectiveness in Trickle-bed Reactors," *AIChE J.*, **24,** 1087 (1978).
Herskowitz, M., and J. M. Smith, "Trickle Bed Reactors: A Review," *AIChE J.*, **29,** 1 (1983).
Hirose, T., "Recent Trend of Studies on Gas-Liquid Cocurrent Packed Column," Symp. Multiphase Concurrent Fixed Beds," Okayama, Japan, 1 (1978).
Hofmann, P. H., "Multiphase Catalytic Packed-bed Reactors," *Catl. Rev. Sci. Eng.*, **17,** 71 (1978).
Kemblowski, Z., and J. Mertl, "Pressure Drop during the Flow of Stokesian Fluids through Granular Beds," *Chem. Eng. Sci.*, **29,** 213 (1974).
Larkins, R. P., R. R. White, and D. W. Jeffrey, "Two-phase Concurrent Flow in Packed Beds," *AIChE J.*, **7,** 231 (1961).
Lockhart, R. W., and R. C. Martinelli, "Proposed Correlation of Data for Isothermal Two-phase, Two-component Flow in Pipes," *Chem. Eng. Prog.*, **45,** 39 (1949).
Matsuura, A., T. Akehata, and T. Shirai, "Friction Factor of Gas-Liquid Concurrent Downflow through Packed Beds," *Kagaku Kogaku Ronbunshu*, **3**(2), 122 (1977).
Midoux, N., M. Favier, and J. C. Charpentier, "Flow Pattern, Pressure Loss, and Liquid Holdup Data in Gas-Liquid Downflow Packed Beds with Foaming and Nonfoaming Hydrocarbons," *J. Chem. Eng. Japan*, **9,** 350 (1976).
Rao, V. G., M. S. Ananth, and Y. B. G. Varma, "Hydrodynamics of Two-phase Cocurrent Downflow through Packed Beds," *AIChE J.*, **29,** 467 (1983).
Rao, V. G., R. S. Raju, M. S. Ananth, and Y. B. G. Varma, "Flow Pattern in Cocurrent Gas-Liquid Downflow in Packed Beds," *Ind. Chem. Eng.*, **23,** 25 (1981).
Saez, A. E., and R. G. Carbonell, "Hydrodynamic Parameters for Gas-Liquid Concurrent Flow in Packed Beds," *AIChE J.*, **31,** 52 (1985).
Sato, Y., T. Hirose, F. Takahashi, and M. Toda, "Pressure Loss and Liquid Holdup in Packed-bed Reactor with Cocurrent Gas-Liquid Downflow," *J. Chem. Eng. Japan*, **6,** 147 (1973).
Satterfield, C. N., "Trickle-bed reactors," *AIChE J.*, **21,** 209 (1975).
Shah, Y. T., *Gas-Liquid-Solid Reactor Design*, McGraw-Hill, New York (1979).
Specchia, V., and G. Baldi, "Pressure Drop and Liquid Holdup in Two-phase Concurrent Flow in Packed Beds," *Chem. Eng. Sci.*, **32,** 515 (1977).
Sweeney, D. E., "A Correlation for Pressure Drop in Two-Phase Cocurrent Flow in Packed Beds," *AIChE J.*, **13,** 663 (1967).
Talmor, E., "Two-phase Downflow through Catalyst Beds," *AIChE J.*, **23,** 868 (1977).
Tuprin, J. L., and R. L. Huntington, "Prediction of Pressure Drop for Two-phase, Two-component Concurrent Flow in Packed Beds," *AIChE J.*, **13,** 1196 (1967).
Weekman, V. W., Jr., and E. Myers, "Fluid Flow Characteristics of Concurrent Gas-Liquid Flow in Packed Beds," *AIChE J.*, **10,** 951 (1964).

Manuscript received Mar. 6, 1987, and revision received July 13, 1987.